J Mater Sci (2007) 42:646–651
DOI 10.1007/s10853-006-1140-2

Crystallization and thermally induced surface relief effects in a $Mg_{65}Cu_{25}Y_{10}$ bulk metallic glass

G. Chen · M. Ferry

Received: 29 March 2004 / Accepted: 17 November 2005 / Published online: 23 November 2006

Abstract The crystallization behaviour of $Mg_{65}Cu_{25}Y_{10}$ bulk metallic glass (BMG) under different reheating conditions was investigated. X-ray diffraction spectrometery (XRD), differential scanning calorimetery (DSC), scanning electron microscopy (SEM) and atomic force microscopy (AFM) were employed to examine the crystallization of different samples and the surface relief generated on as-polished surfaces during heat treatment. Different phase constituents were found in samples that experienced different reheating stages. It is proposed that both the reheating temperature and holding time have a significant effect on the phase constituents. The BMG was found to generate surface corrugations of amplitude 1–2 μm during annealing above its crystallization temperature. Such thermally induced surface relief effects are probably a result of the development of surface stresses generated by volumetric changes associated with crystallization of the residual amorphous phase.

Introduction

Alloy systems based on Mg–Cu were found to be glass formers about two decades ago [1]. Kim et al. [2] reported that melt-spun Mg–Cu–Y ribbons possessed a supercooled liquid region while Inoue et al. [3] demonstrated that amorphous alloys with a composition of $Mg_{65}Cu_{25}Y_{10}$ could be produced in thickness up to 4 mm by conventional mold casting techniques. The glass forming ability (GFA) of Mg–Cu–Y alloys was reported to vary with the content of magnesium, copper as well as yttrium [2–4], and with a maximum at the composition of $Mg_{65}Cu_{25}Y_{10}$.

The production of Mg-based bulk metallic glasses (BMGs) has opened up a new area in the development of high strength, low density alloys. However, Mg–Cu–Y BMGs were found to possess little ductility at room temperature, which is expected to limit the further development of Mg–Cu–Y amorphous systems. A series of subsequent researches [4–15] have focused on the modification of GFA of Mg–Cu–Y and the improvement of its room-temperature mechanical properties by the addition of other alloying elements. However, other elements generally lower the GFA although it was found that thicker as-cast ingots may be obtained by the addition of Ag [13–15].

Linderoh et al. [16] have reported the thermal stability of a $Mg_{60}Cu_{30}Y_{10}$ BMG in the supercooled liquid region using DSC at a heating rate of 20 K/min and found T_g = 408 K and T_x = 458 K where T_g is the glass transition temperature and T_x the crystallization temperature. The transition from an amorphous to fully crystalline state was studied by X-ray diffraction (XRD) as a function of time at specific temperatures in the region between T_g and T_x. These workers subsequently generated a temperature–time–transition (TTT) phase diagram, which was used as the basis for selecting the optimum temperature in the supercooled

G. Chen
School of Materials Science and Engineering,
Jiangsu University, Zhenjiang 212013, P.R. China
e-mail: gchen@ujs.edu.cn

M. Ferry (✉)
School of Materials Science and Engineering, University
of New South Wales, Sydney, NSW 2052, Australia
e-mail: m.ferry@unsw.edu.au

liquid region for carrying out deformation/shaping operations on their Mg-based alloys. Despite this work, little research on the Mg–Cu–Y amorphous system has been reported on the crystallization behaviour in the vicinity of the crystallization temperature. The aim of the present work is to investigate the thermally induced crystallization behaviour of the $Mg_{65}Cu_{25}Y_{10}$ BMG.

Experimental procedures

An alloy of composition $Mg_{65}Cu_{25}Y_{10}$ was produced in ingot form by melting high purity magnesium (99.98 wt.%) and a Cu–Y master alloy in an electrical resistance furnace under argon atmosphere. The Cu–Y master alloy was prepared by arc melting high purity copper and yttrium (99.99 wt.%) in an argon atmosphere. Plate-shaped samples of thickness 2 mm were prepared by a conventional mold casting method. The as-cast plate was cut to produce rectangular samples of size 5 mm × 5 mm × 2 mm. These samples were reheated in a salt bath furnace for various times and temperatures after the bath was stabilised for 10 min at the required temperature. The reheating conditions of the various samples are given in Table 1.

The densities of a range of samples were measured by an Archimedean method and distilled water at 298 K was employed as the medium. A Philips X1400 X-ray diffractometer using Cu Kα radiation was used to examine the phase constituents of the samples under various stages of heat treatment. In order to eliminate the probable influence of surface oxidation, all samples were mechanically polished before carrying out XRD. Differential scanning calorimetry (DSC) was carried out using a Setaram Labsys 16 DSC where the heating rate was 20 K/min. The as-treated surfaces of different samples were examined under scanning electron microscope (SEM) using a Hitachi S4500 field emission gun scanning electron microscope (FEGSEM). The surface relief associated with crystallization was studied by atomic force microscopy (AFM) using a Dimension-3000 AFM. AFM examination was carried out in contact imaging mode in the air and a V-shaped silicon nitride cantilever with a standard pyramidal tip was applied. The microstructures of these samples were then identified using the FEGSEM after mechanical polishing.

Table 1 Reheating temperatures and holding times for various samples

Sample	S1	S2	S3	S4	S5	S6	S7	S8	S9
T (K)	483	483	483	503	503	503	523	523	523
t (min)	3	6	9	3	6	9	3	6	9

Table 2 Densities of various samples

Sample	As-cast glass	S3	S6	As-cast crystalline
Density ($\times 10^3$ kg/m^3)	3.266 ± 0.002	3.269 ± 0.002	3.285 ± 0.002	3.288 ± 0.002

Results and discussion

The densities of various samples are given in Table 2 with an error of measurement of 0.002×10^3 kg/m^3. It is clear that there is very small difference between the densities of different samples, which agrees with the results on other BMGs reported by Inoue et al. [17]. However, it is also clear that the density difference between the fully crystalline sample and the partially crystallized samples is larger than that between the as-cast and partially crystallized samples. Although the Mg_2Cu phase that forms has a relatively high density (3.41×10^3 Kg/m^3 [18]), the density variation of the material during partial crystallization is only slight due to the formation of the residual glass with relatively low density as there is a lower copper content in the this phase compared with Mg_2Cu. It is also well known that that the glass phase has a density of up to 1% less than the corresponding crystalline phase(s) [17].

Figure 1 gives XRD spectra of the as-cast sample (Fig. 1a) and samples heat treated for the indicated conditions. The spectrum in Fig. 1a is indicative of an amorphous state while the peaks in the spectra of the heat treated samples (Fig. 1b–d) indicates a transformation from the modified amorphous phase (probably containing the icosahedral phase, as reported in [19]) to an amorphous phase containing Mg_2Cu and, finally, to Mg solid solution containing Mg_2Cu, $Mg_{24}Y_5$ and Cu_2Y. The XRD results of samples obtained at other temperatures show that the constituents of the reheated samples change from a modified amorphous state (S1) to amorphous and Mg_2Cu (S2 and S3) at 483 K, and from the modified amorphous state (S7) to amorphous and Mg_2Cu and eventually to Mg solid solution containing Mg_2Cu, $Mg_{24}Y_5$ and Cu_2Y (S8 and S9) as the holding time increases at 523 K.

DSC was used to study the progress of crystallization during continuous heating. Figure 2 shows DSC results for various samples. From Fig. 2a it can be seen that the reheating temperatures employed are above

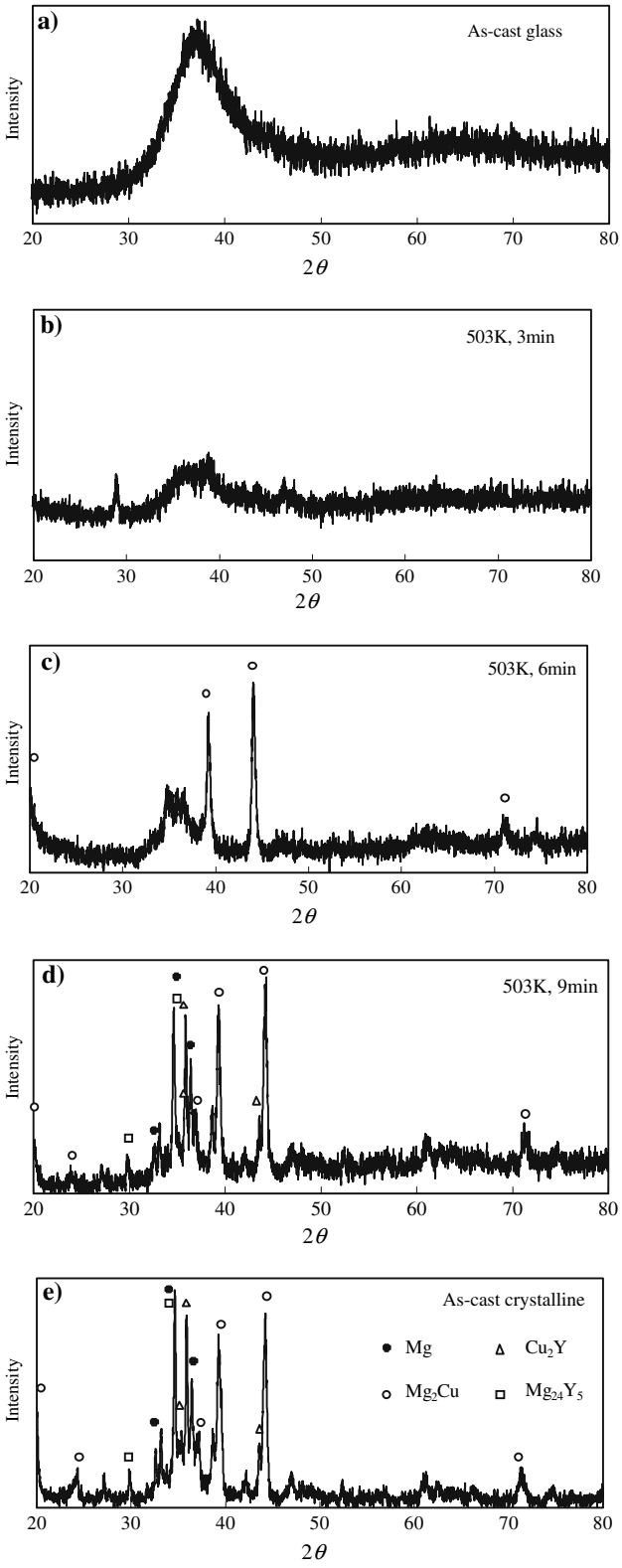

Fig. 1 XRD spectra of: (**a**) as-cast BMG and BMG heat treated at 503 K for (**b**) 3 min (specimen 4), (**c**) 6 min (specimen 5) and (**d**) 9 min (specimen 6). The as-cast alloy in the fully crystalline state is given in (e)

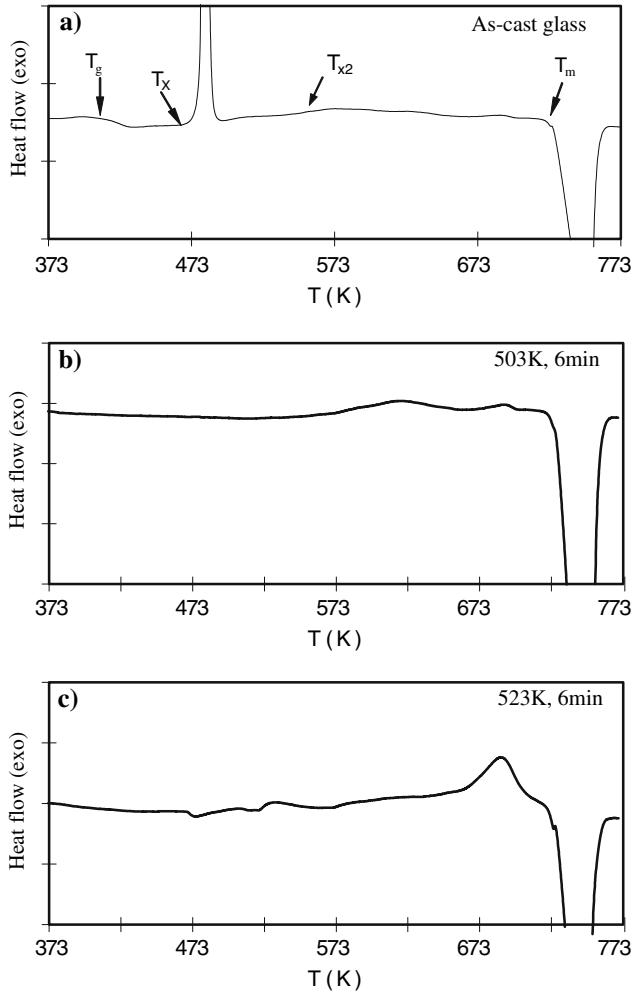

Fig. 2 DSC patterns of: (**a**) as-cast BMG and BMG heat treated for 6 min at: (**b**) 503 K (specimen 5) and (**c**) 523 K (specimen 8)

the crystallization temperature, i.e. the onset temperature of crystallization during reheating. However, comparison of Figs. 2a and b shows that samples with different starting structures undergo different phase transitions during heating. FEGSEM was used to examine the microstructure of different samples. Figure 3 gives a series of SEM micrographs during various stages of heat treatment. It is clear in Fig. 3a that the amorphous starting material shows no surface detail other than oxide films which form during casting as reported by Men et al. [12]. The fully crystalline structure, Fig. 3b, obtained from a large as-cast crystalline ingot, is different from Fig. 3a with the former showing eutectic grains with some oxides, as shown in Fig. 3a, in the as-cast sample. Figures 3c and d show the presence of Mg_2Cu particles which were found to coarsen with increasing temperature. The microstructures observed by SEM correlate closely with the phases identified by XRD.

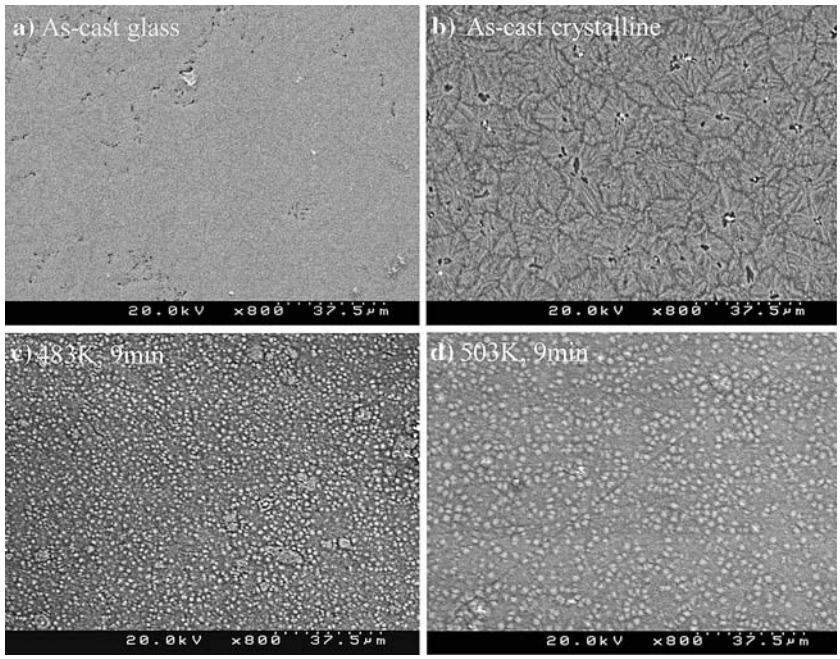

Fig. 3 SEM micrographs of as-cast (**a**) BMG and (**b**) fully crystalline alloy, and BMG heat treated for 9 min at (**c**) 483 K (specimen 3) and (**d**) 503 K (specimen 6)

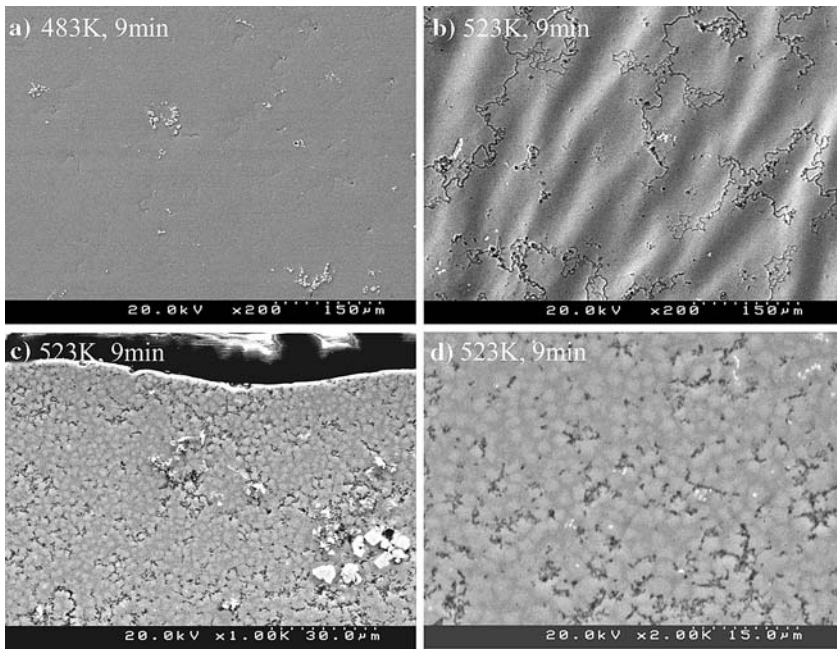

Fig. 4 SEM micrographs of the as-polished surface of the BMG heat treated for 9 min at (**a**) 483 K and (**b**) 523 K; (**c**) and (**d**) are cross-sections of the sample heat treated for 9 min at 523 K

An interesting aspect of the heat treatment of the as-cast BMG was the generation of surface corrugations on as-polished samples during heating. Samples 6, 8, and 9 were found to consistently develop these surface features during heat treatment. Figure 4 shows a series of SEM micrographs of samples 3 and 9. Figure 4a and b are as-polished and as-polished and heat treated surfaces, respectively, clearly showing the formation of banded features on the surface after heat treatment. Figures 4c and d are through-thickness SEM micrographs which show very little microstructural difference between the surface region and the bulk of the material. AFM was used to examine the surface topography of the as-cast and polished samples during various stages of heat treatment. Figure 5 gives a typical AFM image of the surface relief that is generated by the heat treatment which clearly shows the surface corrugations generated by the heat treatment. Figure 5a shows a band height of 1–2 μm with a band width of 20–50 μm. An interesting feature of the AFM images of

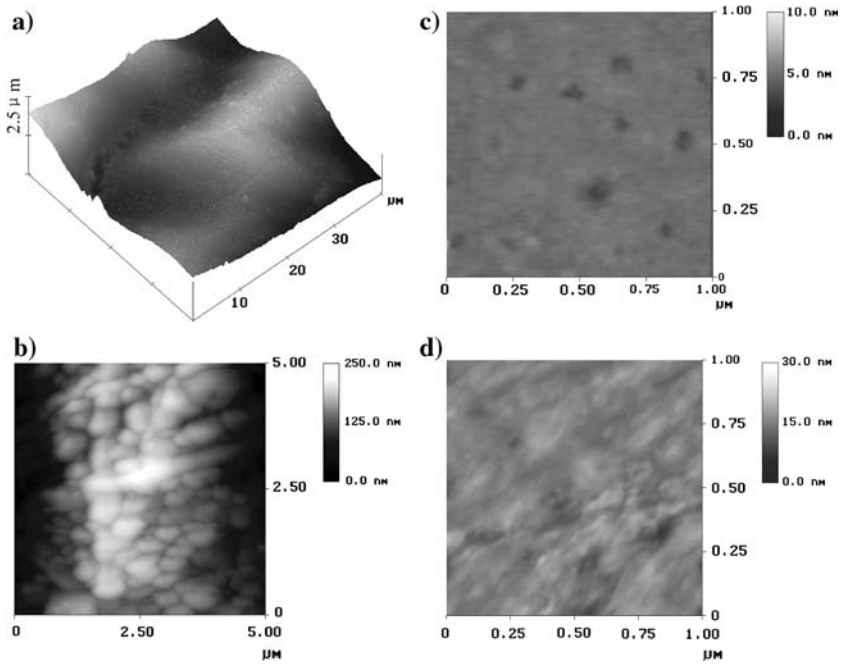

Fig. 5 AFM surface images of: (**a**) and (**b**) as-cast and polished BMG after heat treatment for 9 min at 523 K; (**c**) as-cast BMG, and (**d**) as-polished surface of BMG

the ridged regions is the presence of clustered features on the surface (Fig. 5b) which were absent in the as-cast (Fig. 5c) and as-polished samples (Fig. 5d).

The formation of the Mg_2Cu phase during heat treatment of an as-cast $Mg_{60}Cu_{30}Y_{10}$ BMG between the glass transition temperature (T_g = 408 K) and the crystallization temperature (T_x = 458 K) was reported by Linderoh et al. [16], which is confirmed in the present work. However, micro-sized particles (~2 μm in diameter) rather than nanocrystalline Mg_2Cu particles were formed in the present alloy after reheating and isothermally annealing above the crystallization temperature (T_x = 479.4 K). As the reheating temperature is increased, it is expected that both the nucleation rate and growth rate of the crystalline phase will increase, which will allow Mg_2Cu particles to form readily from the amorphous phase with the high temperatures resulting in further particle coarsening. Consequently, as temperature is increased, the structure progressively changed from the amorphous state to a modified amorphous state, then to an amorphous phase containing Mg_2Cu particles, and finally, to a crystalline state containing various phases (Fig. 1d). There is a second crystallization temperature, T_{x2}, which is above 523 K (Fig. 2a) and indicates that complete crystallization of the BMG does not occur unless longer annealing times are used to completely crystallize the residual amorphous phase.

An interesting aspect of the heat treatment of the as-cast glass is the generation of surface relief effects (Fig. 5a). However, there was no significant difference between the SEM micrographs that show only the Mg_2Cu phase in the XRD patterns and samples 6, 8 and 9 besides a small size difference of the Mg_2Cu particles. Further analysis of both the different phases observed by SEM and XRD spectra indicates that the residual amorphous phase was consumed in samples 6, 8 and 9. Therefore, the generation of these surface corrugations is likely to be a result of crystallization of the residual amorphous phase rather than the formation of Mg_2Cu phase. Table 2 shows that the density of the as-cast crystalline sample is largest with the density difference between the fully crystalline sample and the partially crystallized samples being larger than that for the as-cast and partially crystallized samples. It is possible, therefore, that a given sample will undergo a compressive stress in the vicinity of the sample surface during crystallization of the residual amorphous phase. If these compressive stresses are large enough, the surface regions will deform to produce these unusual surface rumpling effects.

On a final note, the generation of surface irregularities of amplitude 1–2 μm during crystallization of the Mg-base BMG may be problematic, considering the recent work on precision forming of BMGs for the production of nanodevices [20]. It was shown that Pd-base BMGs have exceptional microformability through their ability to replicate very fine and complex surface features of a die. However, crystallization-induced surface rumpling during or after forming must be avoided, that is, forming must be carried out below the crystallization temperature.

Conclusions

The crystallization behaviour of an as-cast $Mg_{65}Cu_{25}Y_{10}$ BMG was studied by heating in the vicinity of its crystallization temperature. During isothermal annealing at 503 K, crystallization was found to proceed as follows: fully amorphous to a modified amorphous phase to a residual amorphous phase containing Mg_2Cu particles and, finally, to the fully crystallized state. Heat treatment of the as-cast BMG generated surface corrugations on an as-polished surface. The generation of this surface relief is likely to be a result of crystallization of the residual amorphous phase that generates surface compressive stresses as a result of the density differences between the crystalline and amorphous phases.

Acknowledgements One of the authors, Dr Gang Chen, would like to acknowledge the School of Materials Science and Engineering, UNSW for provision of research facilities and the China Scholarship Council for the financial support. The authors gratefully thank John Sharp for the DSC examination and Bülent Gun and Kevin Laws for the provision of samples.

References

1. Sommer F, Bucher G, Predel B (1980) J Phys Coll C8:563
2. Kim SG, Inoue A, Masumoto T (1990) Mater Trans Jim 31:929
3. Inoue A, Kato A, Zhang T, Kim SG, Masumoto T (1991) Mater Trans Jim 32:609
4. Eldrup M, Pedersen AS, Ohnuma M, Pryds N, Linderoth S (2000) J Metastable Nanocryst Alloys 8:123
5. Liu W, Johnson WL (1996) J Mater Res 11:2388
6. Ohnuma M, Linderoth S, Pryds N, Eldrup M, Pedersen AS (1999) Mat Res Soc Symp Proc 554:119
7. Ohnuma M, Pryds N, Linderoth S, Eldrup M, Pedersen AS, Pedersen JS (1999) Scripta Metall 41:889
8. Kang HG, Park ES, Kim WT, Kim DH, Cho HK (2000) Mater Trans Jim 41:846
9. Linderoth S, Pryds NH, Ohnuma M, Pedersen AS, Eldrup M, Nishiyama N, Inoue A (2001) Mater Sci Eng A 304–306:656
10. Murty BS, Hono K (2000) Mater Trans Jim 41:323
11. Pryds NH, Eldrup M, Ohnuma M, Pedersen AS, Hattel J, Linderoth S (2000) Mater Trans Jim 41:1435
12. Men H, Hu ZQ, Xu J (2002) Scripta Mater 46:699
13. Amiya K, Inoue A (2000) Mater Trans Jim 41:1460
14. Park ES, Hang HG, Kim WT, Kim DH (2001) J Non Crystalline Solids 27:154
15. Ma H, Ma E, Xu J (2003) J Mater Res 18:2288
16. Linderoh S, Pryds N, Eldrup M, et al. (2001). In: Inoue A et al. (ed) Supercooled liquid, bulk glassy and nanocrystalline states of alloys (Materials Research Society Symposium Proceedings 644), p L4.1.1
17. Inoue A (2000) Acta Mater 48:279
18. Gingl F, Selvam P, Yvon K (1993) Acta Cryst B49:201
19. Köster U, Zander D, Jainlewing R (2001) In: Inoue A et al. (ed) Supercooled liquid, bulk glassy and nanocrystalline states of alloys (Materials Research Society Symposium Proceedings 644), p L5.8.1
20. Saotome Y, Itoh K, Zhang T, Inoue A (2001) Scripta Mater 44:1541